Ceramics-Silikáty 61 (2), 91-98 (2017)
www.ceramics-silikaty.cz doi: 10.13168/cs.2017.0002

PROCESSING OF CONCENTRATED AQUEOUS ZIRCONIA-BIOGLASS SLIPS BY SLIP CASTING

BELTINA LEÓN, MARÍA P. ALBANO, FRANCO M. STÁBILE AND LILIANA B. GARRIDO

Centro de Tecnología de Recursos Minerales y Cerámica (CETMIC),
C. C. 49 (B1897ZCA) M. B. Gonnet, Provincia de Buenos Aires, Argentina

#E-mail: palbano@cetmic.unlp.edu.ar

Submitted December 22, 2016; accepted January 31, 2017

Keywords: Y-TZP- bioglass suspensions, Zeta potential, Rheological properties, Slip casting

3 mol% yttria-partially stabilized zirconia (Y-TZP) powder and a sol-gel derived $CaO–P_2O_5–SiO_2$ (64S) bioglass, were used to produce Y-TZP- bioglass slip cast compacts. The rheological properties of concentrated aqueous Y-TZP-64S suspensions prepared with two different glass contents: 10.5 vol% and 19.9 vol%, and ammonium polyacrylate (NH_4PA) as dispersant, were investigated and compared with those of Y-TZP. The density of green cast samples was related to the degree of slip dispersion. The substitution of Y-TZP by 64S glass in the mixtures resulted in greater adsorption of NH_4PA; however, the viscosity and yield stress values of Y-TZP-64S slips were higher than those of Y-TZP ones for the solid loadings studied. The increase in the glass content from 10.5 to 19.9 vol% increased the viscosity and yield stress values. The presence of 64S glass in the mixtures resulted in a less dense packing of cast samples.

INTRODUCTION

3 mol% yttria-partially stabilized zirconia (Y-TZP) ceramics are used in dental clinical implants owing to their excellent mechanical properties and biocompatibility [1, 2]. Y-TZP bioceramics are used primarily in the development of prosthesis or parts in restorations [3, 4]. All-ceramic dental restorations are attractive to the dental community because they provide higher strength, abrasion resistance, better biocompatibility and aesthetics, as compared with metal and resin restorations [5, 6].

Zirconia ceramics are usually fabricated via solid state sintering at high temperatures of around 1500-1600°C [1, 7], which is a relatively expensive fabrication method that increases production costs. In order to lower the sintering temperature of ZrO_2, additives are deliberately introduced such as Fe_2O_3, SiO_2, Al_2O_3, TiO_2, and others [8]. There are some reports [9,10] concerning the effect of bioglass additives on the sintering behaviour of ZrO_2; some glass compositions result in improved densification of ZrO_2 via liquid phase sintering, other ones enhanced the ZrO_2 solid state sintering.

Commonly, Y-TZP-bioglass components are produced by conventional powder processing techniques which involve mixing, pressing and subsequent sintering. However, green compacts obtained by slip casting have higher microstructural homogeneity and near-net-shaping that reduce the post sintering machining operations and the production costs [11, 12]. The colloidal processing of Y-TZP-bioglass by slip casting requires the preparation of stable concentrated aqueous suspensions of the ceramic powders. At high solids loading, relatively low slip viscosity can only be achieved in the presence of an optimum dispersion state of particles. Anionic polyelectrolytes such as NH_4PA are commonly used as dispersant of ceramic powders in aqueous solution [13]. The polyelectrolyte adsorbs at the solid-liquid interface producing repulsive interactions (electrostatic and steric) between the particles [14].

Various bioactive glasses have been developed, many of which still rely on the 45S5 bioglass discovered by Hench [15]. However, one of the main problem associated with this glass is its high dissolution rate [16] due to its high alkali content; thus, the preparation of stable concentrated aqueous Y-TZP-45S5 suspensions for slip casting is strongly limited by the solubility of 45S5 bioglass. In order to reduce the aqueous dissolution rate of the glass, the present investigation used an alkali-free bioglass in the $CaO–P_2O_5–SiO_2$ system, formed by the sol-gel technique, with a low level of calcium cations in its composition: 64 mol% SiO_2, 26 mol% CaO, 10 mol% P_2O_5 (64S), as an additive for Y-TZP.

In this study, the rheological properties of concentrated aqueous Y-TZP-64S suspensions prepared with two different glass contents, 10.5 vol% (5 wt%) and 19.9 vol% (10 wt%), and NH_4PA as dispersant were investigated and compared with those of Y-TZP. In addition, the density of green cast samples was related to the degree of slip dispersion.

EXPERIMENTAL

Raw materials and powder processing

3 mol% yttria- partially stabilized zirconia (Y-TZP) (Saint-Gobain ZirPro, Chine) powder was used in this study. The sol-gel synthesis of the glass in the CaO–P_2O_5–SiO_2 system with composition : 64% SiO_2, 26% CaO and 10% P_2O_5 (mol%) was performed as follows: initially, tetraethoxysilane (TEOS, Aldrich) was added to 0.1 M nitric acid and the mixture was allowed to react for 60 min for the acid hydrolysis of TEOS. Then, a series of reagents were added in the following sequence: triethylphosphate (TEP, Aldrich) and calcium nitrate tetrahydrate (Aldrich), allowing 45 min for each reagent to react completely. After the final addition, mixing was continued for 1 h for the completion of the hydrolysis. The resultant solution was kept in a sealed container for 10 days at room temperature to allow gelation to occur and subsequently heated at 70 °C for an additional 3 days. Afterwards, the water was removed and a small hole was inserted in the lid to allow the leakage of gases while the gel was heated at 120°C for 2 days. The dried gel was then heated at 700°C for 24 h to stabilize the glass and eliminate residual nitrates. The stabilized glass powder was milled in an attrition mill using 1.6 mm zirconia balls during 48 hours. This bioglass powder subsequently referred as 64S was used for the experiments presented in this study; its measured density was 2.70 g/cm^3.

Y-TZP-64S compositions with two different 64S contents: 10.5 vol% (5 wt%) and 19.9 vol% (10 wt%) were used to prepare the ceramics. A commercial ammonium polyacrylate solution (Duramax D 3500, Rohm & Haas, Philadelphia PA) was used as deflocculant. 35 vol% aqueous Y-TZP and Y-TZP-64S suspensions with the different compositions and various amounts of deflocculant were prepared by suspending particles in deionized water via 40 min of ultrasound; when it was necessary the pH was manually adjusted to be maintained at 9 with ammonia (25 %). In addition, slips with the optimum NH_4PA concentration and a solid content of 43 vol% were prepared at pH 9 to study the influence of the solid loading on the rheological properties.

Slips were cast in plaster molds into disks of diameter 1.85 cm. The consolidated disks were dried slowly in air for 24 h at room temperature and 24 h at 100°C.

Characterization techniques

The 64S glass powder was characterized by X-ray diffraction (XRD) analysis (Philips 3020 equipment) using Cu-Kα radiation with Ni filter at 40 kV–20 mA. The particle size distribution of the Y-TZP and glass powders were measured using a Mastersizer 2000 (Malvern Instruments, UK). The morphological features of the powders were examined by scanning electron microscopy (SEM) (JEOL, JSM-6360).

The aqueous dissolution behaviour of 64S glass was studied by measuring the pH of 20 wt% slips as a function of immersion time. Zeta potential against pH curves were determined with an instrument Zetasizer nano ZS (Malvern Instruments, UK) for 0.05 vol% slips of Y-TZP and 64S powders in the pH range of 2-10.5. The pH adjustment was achieved with HCl or NH_4OH solutions. The pH was measured with a pH meter calibrated with buffer solutions (pH 4, 7 and 10, Merck, Germany). Zeta potential versus pH curves were determined for 0.05 vol% slips of Y-TZP, 10.5 and 19.9 vol% 64S with the optimum amount of NH_4PA in the pH range 2-10.5.

Steady state flow curves of the different Y-TZP and Y-TZP-64S slips were performed by measuring the steady shear stress value as a function of shear rate in the range of shear rates between 0.5 to 542 s^{-1}using a concentric cylinder viscometer (Haake VT550, Germany) at 25°C. A coaxial cylinder system with two gaps (sensor system NV Haake) was used. As soon as stationary conditions were reached at each shear rate, the shear rate increased in steps up to the maximum value and then decreased. The density of the green compacts was determined by the Archimedes method using mercury displacement.

RESULTS AND DISCUSSION

Powder characterization

The XRD patterns of the 64S glass (Fig. 1) exhibited a broad peak at 30.2°2θ corresponding to the formation of wollastonite $CaSiO_3$ (JCPDS 42-0547) superimposed on an amorphous halo. The presence of this peak was attributed to the partial crystallization of the glass, which took place during the calcination process at 700°C [17].

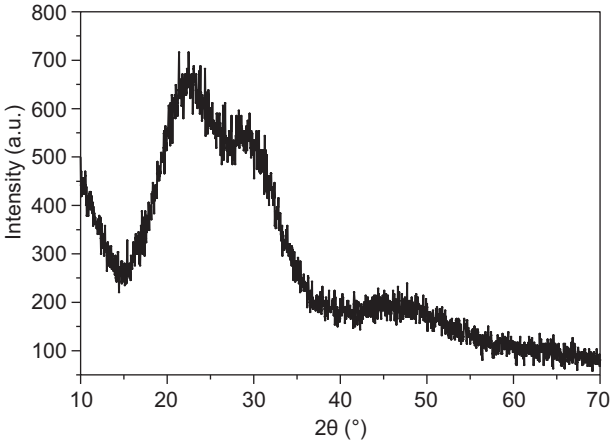

Figure 1. XRD patterns of the 64S glass.

Figure 2 shows the particle size distribution curves of the Y-TZP and 64S glass powders. A narrow particle size distribution with particle sizes between 1 and 13 μm was found for the glass; the more frequent particle diameter was 3.80 μm. A bimodal distribution curve with particle sizes > 0.05 and < 1.5 μm was found for

Y-TZP, the more frequent particle diameters (0.14 and 0.48 μm) were lower than that of the glass. SEM images of the glass and Y-TZP powders (Fig. 3) confirmed the measured particle sizes ranging from 1 to 13 μm for the glass (Fig. 3b), while submicron particle sizes were found for Y-TZP powder (fig. 3a); the shape of the glass particles showed smooth and sharp edges.

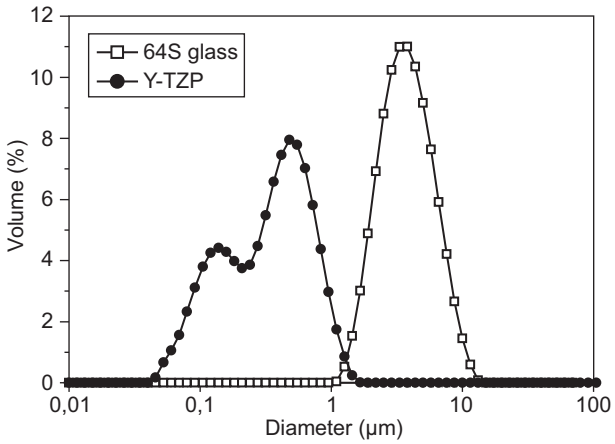

Figure 2. Particle size distribution curves of the Y-TZP and 64S glass powders.

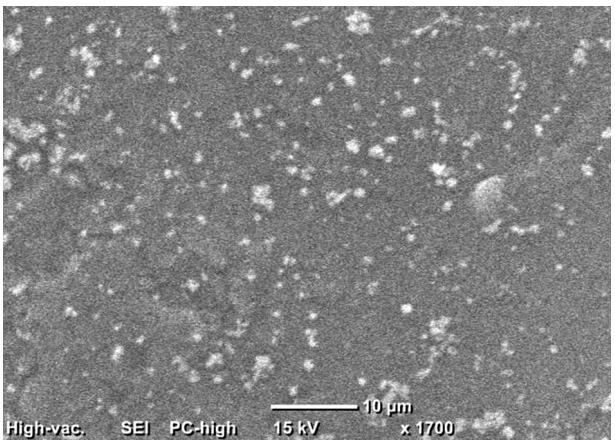

a) Y-TZP

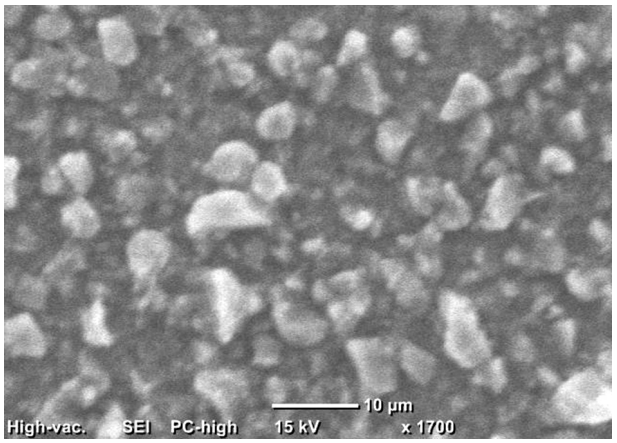

b) 64S glass

Figure 3. SEM micrographs of different powders: a) Y-TZP, b) 64S glass.

Figure 4 shows the pH as a function of the immersion time for 20 wt% 64S slips. The respective curve for 20 wt% 45S5 slips determined in our previous study [18] is also shown for comparison. For the 64S glass studied, a slight increase in pH during 2 h 30 min of immersion in aqueous solution from 7.35 (the initial pH of water) to 8.37 was found, while an important increase in pH to 11.50 was found for the 45S5 immediately after immersion.

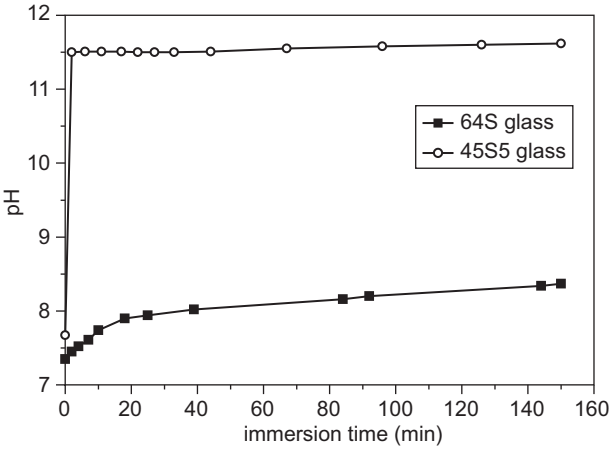

Figure 4. pH as a function of the immersion time for 20 wt% slips of different glasses: 64S, 45S5 (data from Stábile et al., 2016).

Silicate glasses are composed of silica tetrahedral connected by Si–O–Si binding oxygen bonds [19]. Silicon is the glass network forming atom, sodium and calcium are network modifiers which forms non-bridging oxygen bonds such as $Si–O^- Na^+$ /Ca^{2+} bonds [20]. The phosphorous is present in the glass in an orthophosphate environment with charge balanced by sodium and or/ calcium [20]. The immersion of the 45S5 glass in water produces a rapid cation exchange of Ca^{2+} and/or Na^+ with H^+ from the solution, creating silanol bonds (Si–OH) on the glass surface and OH^- in the aqueous solution [19]. Thus, the pH rise upon the 45S5 immersion in the aqueous solution could be explained by the following ion exchange reaction on the glass surface:

$$Si–O^- Na^+ + H^+ + OH^- \rightarrow Si–OH + Na^+ + OH^- \quad (1)$$

A similar exchange reaction occurs for Ca^{2+}; phosphorous is also releases to the solution [21]. As reported in our previous study [18], the nucleation of amorphous calcium phosphate on the 45S5 surface occurred upon its immersion in water. The amorphous calcium phosphate formation could be interpreted by the bio-mineralization mechanism proposed by Hench [22].

Glass composition is the variable that has the greatest influence on its dissolution rate [15]. The lower amount of modifiers cations and consequently the higher proportion of bridging oxygen bonds for the 64S glass with respect to 45S5 glass resulted in a more connected network which was less prone to dissolution. Thus, the

aqueous dissolution of 64S powder produced a lower increase in pH (Fig. 4) and consequently a lower Ca^{2+} and PO_4^{3-} ions concentration in aqueous solution. According to Goel et al. [23], at pH < 9.0 calcium phosphate precipitation does not occur after water immersion due to the low amounts of Ca^{2+} and PO_4^{3-} ions released, therefore in this study a Ca–P layer on the 64S powder surface is not expected.

Figure 5 shows the zeta potential versus pH curves of the different powders. The isoelectric point (IEP) of Y-TZP powder was found to be about 2.50. The surface charge of the 64S powder was negative in the whole pH range studied; a slightly increase in the negative surface charge of the glass with increasing pH was observed. The glass surface mainly consists of silanol (Si–OH) and $\equiv CaOH_2^+$ sites and a lower amount of $\equiv PO^-$ surface groups [18]. At alkaline pH, the Si-OH and $\equiv CaOH_2^+$ sites loss a proton producing $Si–O^-$ and $\equiv CaOH^0$ sites which imparts a low negative surface charge. On the contrary, the negative zeta potential of the Y-TZP powder strongly increased with increasing pH having higher values in the pH region 5-10.5 compared with the 64S glass. The magnitudes of the negative zeta potential at pH 9 were -41.59 and -26.21 mV for Y-TZP and 64S glass, respectively.

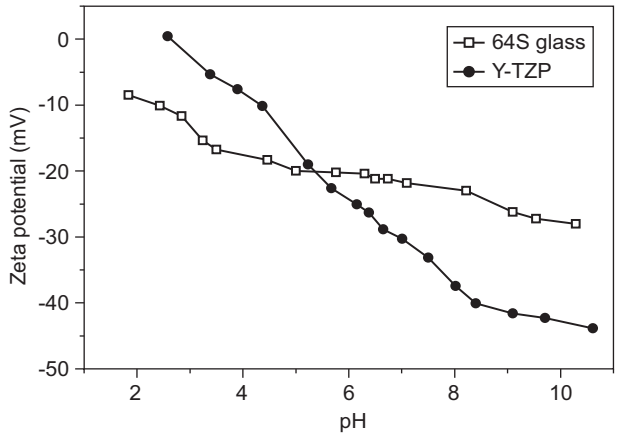

Figure 5. Zeta potential versus pH curves of the different powders: Y-TZP and 64S glass.

Rheological Properties

The NH_4PA concentration that gave slips with the lowest viscosity (optimum concentration), was determined by measuring the apparent viscosity of 35 vol% slips at a shear rate of 542 s^{-1} as a function of the amount of NH_4PA solution added at pH≈ 9 for the slips with the different compositions (fig. 6). The optimum NH_4PA concentration was 0.20, 0.52 and 0.38 wt% (dry weight basis of powder) for Y-TZP, 10.5 and 19.9 vol% 64S slips, respectively.

The ammonium polyacrylate dissociates according to the following reaction:

$$RCOONH_4 \rightarrow RCOO^- + NH_4^+ \quad (2)$$

Since the degree of dissociation was nearly 1 at pH values ≥8.5 [13,14], the polymer charge is negative at those pH values. As it was previously shown in the zeta potential curves (Fig.5), the Y-TZP powder had a high negative zeta potential value at pH 9, therefore an unfavourable electrostatic interaction between the $RCOO^-$ groups of the deflocculant and the Y-TZP particle surface was expected. At pH 9, the electrostatic repulsion between the NH_4PA-adsorbed Y-TZP particles and the polymer in solution limited adsorption to low amounts; as a consequence, a low optimum NH_4PA concentration for Y-TZP slips was measured.

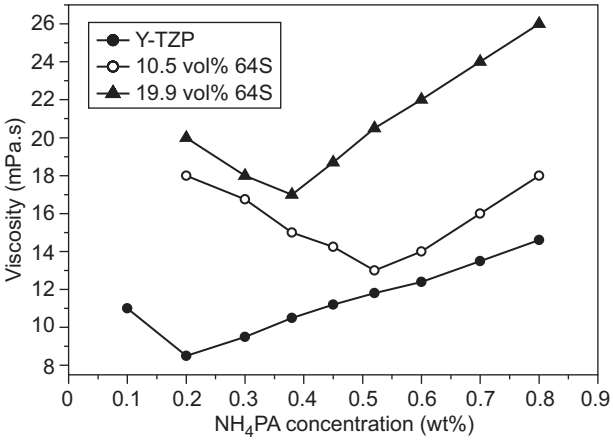

Figure 6. Apparent viscosity of 35 vol% slips at a shear rate (γ) of 542 s^{-1} as a function of the amount of NH_4PA solution added at pH≈ 9 for the slips with the different compositions.

The substitution of Y-TZP by 10.5 vol% 64S in the mixtures decreased the magnitude of the negative zeta potential at pH 9 (fig. 5); as the 10.5 vol% 64S powder surface had more positive sites at which the NH_4PA could be adsorbed a higher adsorption of the anionic polymer with respect to Y-TZP was expected. Thus, the optimum NH_4PA concentration increased from 0.20 for Y-TZP to 0.52 wt% for 10.5 vol% 64S. However, the optimum NH_4PA concentration slightly decreased with increasing the 64S content in the mixtures from 10.5 to 19.9 vol% (fig. 6). Although the substitution of Y-TZP by 19.9 vol% 64S decreased the negative surface charge of the mixture, a lower polymer adsorption of the 19.9 vol% with respect to 10.5 vol% 64S was found. This behaviour could be explained taking into account the particle size of the 64S glass powder. Since the 64S glass powder had particles with greater sizes and consequently lower specific surface area with respect to Y-TZP (Figs. 2 and 3), the substitution of Y-TZP by a high vol% of 64S increased the particle size of the mixture and decreased the amount of NH_4PA adsorbed. Thus, the reduction of the magnitude of the negative zeta potential of 19.9 vol% compared to 10.5 vol% 64S was overcompensated by an increase in the particle size of the mixture, resulting in a lower NH_4PA adsorption.

For all the compositions, the viscosity had different values at the whole range of NH_4PA solution added (Fig. 6). At pH 9, the suspensions with the optimum NH_4PA concentration were stabilized; thus, they were dominated by repulsive forces. The adsorption of the negatively charged polyelectrolyte enhanced the negative surface charge of the powders; in addition, the polyelectrolyte adsorbs in a stretched-out configuration which results in long-range steric interactions of the NH_4PA at the solid-liquid interface [24]. These two effects increased the electrosteric repulsion between particles, consequently the slip viscosity attained the minimum value (Fig. 6).

Polymer additions over the optimum NH_4PA concentration increased the viscosity due to an excess of polymer in solution (fig.6). For polymer additions lower than the optimum NH_4PA concentration, the incomplete adsorption resulted in lower electrostatic repulsion between particles forcing particles together, thereby flocculation occurred (Fig. 6).

The change in pH during the aqueous colloidal processing of 35 vol% Y-TZP -64S slips with the optimum amount of NH_4PA was measured. The pH vs. the solid concentration from 0 to 3.95 g/ml (35 vol%) curve is presented in fig. 7. Similar pH vs. solid concentration curves were found for 10.5 and 19.9 vol% 64S slips. The addition of 0.5 g/ml of the mixture to the aqueous solution with NH_4PA produced a pH increase from 7.3 to 8.8 and 8.9 for 10.5 and 19.9 vol% 64S, respectively. A lesser increase in pH with further increasing the solid concentration was found (lower slope of the pH vs. solid concentration curve), reaching a pH value of 9.0 and 9.1 for 1.5 g/ml of 10.5 and 19.9 vol% 64S, respectively.

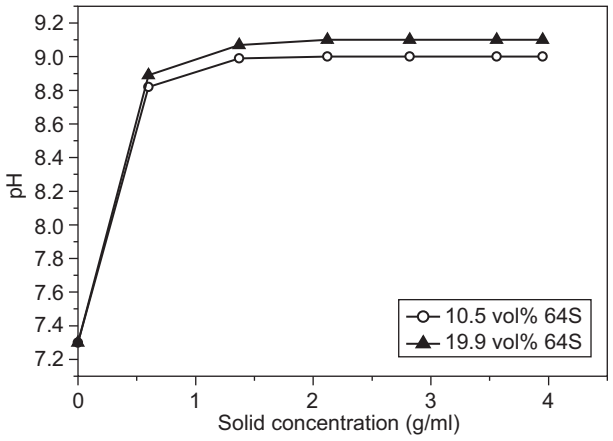

Figure 7. pH as a function of the solid concentration for 35 vol% Y-TZP-64S slips with the optimum amount of NH_4PA.

The increase in pH with the addition of 0.5 g/ml mixture was attributed to the Ca^{2+}/ H^+ exchange reaction at the glass solution interface (eq. 1); however, this pH increase was markedly lower than that observed during the aqueous colloidal processing of 45S5 glass (pH 12) [18]. Thus, the exchange reaction rate at the glass solution interface was significantly reduced by using the composition 64S glass in the present study. Since the pH of the aqueous 10.5 and 19.9 vol% 64S slips spontaneously reached a value of 9.0 and 9.1, respectively, with the addition of a low solid concentration, the addition of ammonia was not necessary. On the contrary, for the aqueous colloidal processing of Y-TZP slips with 0.20 wt% NH_4PA the addition of a low amount of Y-TZP powder produced a decrease in pH, in order to adjust the pH at 9 a low quantity of diluted ammonia should be added.

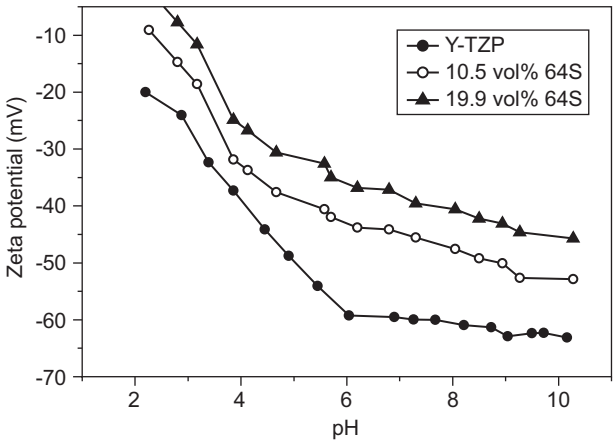

Figure 8. Zeta potential versus pH curves of different slips: Y-TZP, 10.5 and 19.9 vol% 64S with the optimum amount of NH4PA solution added.

Figure 8 shows the zeta potential versus pH curves of different slips: Y-TZP, 10.5 and 19.9 vol% 64S with the optimum amount of NH_4PA solution added. The adsorption of NH_4PA shifted the pH_{IEP} of Y-TZP (fig. 5) from 2.50 to a pH value lower than 2 (Fig. 8); the IEPS of the 10.5 and 19.9 vol% 64S mixtures with NH_4PA were found to be lower than 2. The adsorption of the polyelectrolyte on the Y-TZP powder resulted in a markedly increase in the magnitude of the negative zeta potential in the pH range 2-10.5 (figs. 5 and 8). The negative zeta potential values of the Y-TZP slips with the optimum amount of NH_4PA solution added were higher than those of the 10.5 and 19.9 vol% 64S mixture in the whole range of pH studied. The presence of 64S glass in the mixtures increased the Ca^{2+} concentration in the aqueous solution (eq. 1), as the ionic strength increased the negative surface charge of the mixture decreased due to the large compression of the double layer [14]. Consequently, the substitution of Y-TZP by 64S in the mixtures decreased the negative surface charge of the slips with NH_4PA at pH 9 (Fig. 8).

The decrease in the magnitude of the negative zeta potential in the pH range 2-10.5 with increasing 64S glass content from 10.5 to 19.9 vol% was attributed to the lesser amount of NH_4PA adsorbed. As the 64S concentration increased from 0 to 19.9 vol%, the

negative zeta potential value in the pH range 2-10.5 decreased. The zeta potential values at pH 9 were –62.90, –51.00 and –44.00 mV for Y-TZP, 10.5 and 19.9 vol%, respectively.

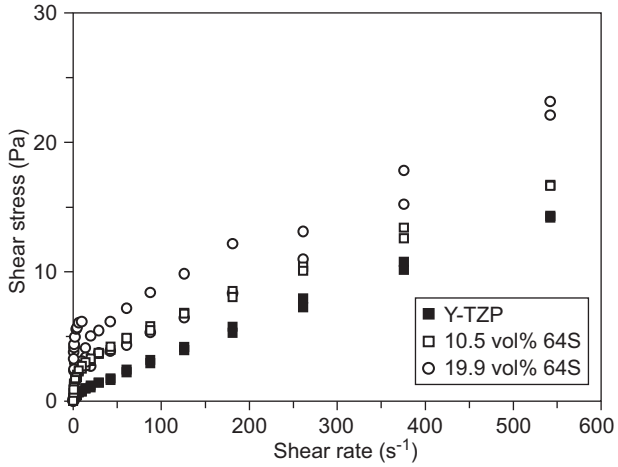

Figure 9. Flow curves of shear stress versus shear rate for 43 vol% slips with the optimum amount of NH_4PA solution added at pH≈9.

Figure 9 shows the flow curves of shear stress versus shear rate for 43 vol% slips with the optimum amount of NH_4PA solution added at pH≈9. The slips exhibited a yield stress followed by a shear thinning flow. The measured flow curves were satisfactorily fitted with the Casson model at the whole range of shear rates. The Casson model equation is:

$$\tau^{1/2} = \tau_0^{1/2} + (\eta_p \gamma)^{1/2} \quad (3)$$

where τ is the shear stress, τ_0 is the yield stress, η_p represents the limiting viscosity at a high shear rate range and γ is the shear rate. The effect of 64S glass content on the apparent viscosity at 542 s^{-1} and τ_0 value, are respectively shown in Figures 10a and 10b, for 35 and 43 vol% stabilized slips at pH≈ 9. The viscosity increased with increasing the 64S glass content in the mixtures (fig. 10a), a greater slope of the viscosity vs. 64S content curve with increasing solid loading was found. As the 64S concentration increased from 0 to 19.9 vol%, the viscosity of 35 and 43 vol% slips respectively increased from 8.50 to 17.00 mPa.s and 27.00 to 54.00 mPa.s. When the solid content increases particles approach each other and overlap their electrical double layers [25] reducing the repulsion between particles; in addition to the electrostatic effect the amount of entrapped liquid (not available for flow) within the aggregated particles increases. These two effects contributed to increase the slip viscosity with increasing solid loading.

In a flocculated suspension the attraction between particles form floc groups which difficult the slurry flow [14]; the τ_0 value increases with increasing the aggregation between particles and consequently the degree of slip flocculation. An important increase in the slopes of the τ_0 vs. 64S content curves with increasing solid loading was found for the slips with different compositions (Fig. 10b); thus, the increase in the solid concentration had more effect on the τ_0 than on the viscosity values.

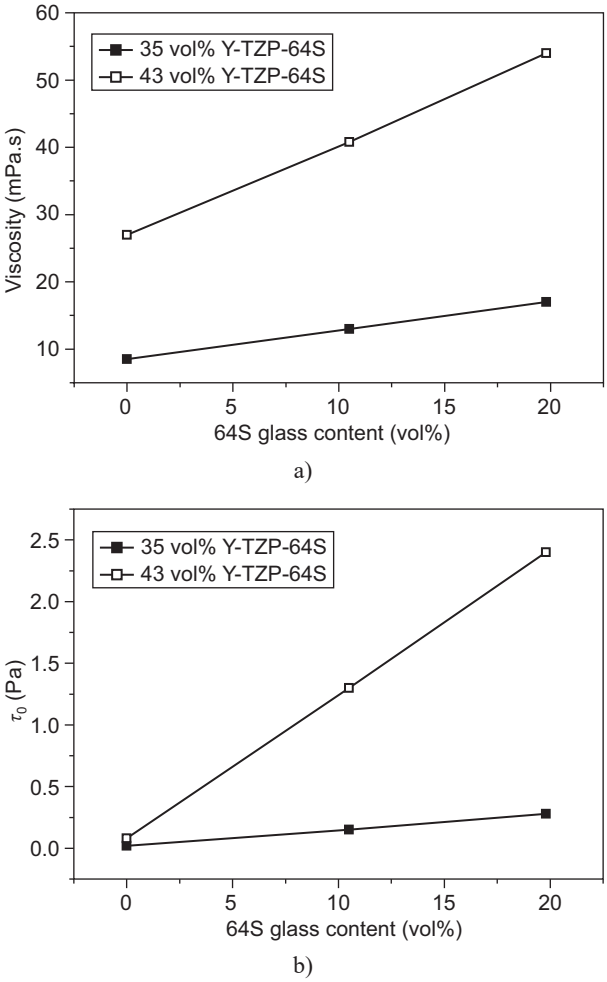

Figure 10. Viscosity at 542 s^{-1} (a) and τ_0 (b) versus the 64S glass content for stabilized slips at pH≈ 9 with different solid loading.

The τ_0 values of 35 vol% slips prepared from Y-TZP and 19.9 vol% 64S, respectively increased from 0.02 to 0.28 Pa; while the τ_0 values of 43 vol% slips markedly increased from 0.08 to 2.40 Pa with increasing the 64S content from 0 to 19.9 vol%. The increase in the yield stress with increasing solid loading was attributed to a higher frequency of collisions between separate particles, increasing the number of flocs and consequently the resistance to flow. Therefore, for the different slip compositions studied, the differences in the viscosity and τ_0 values tended to be more pronounced with increasing the solid loading. Thus, the difference in the viscosity and τ_0 values between both slip concentrations became larger with increasing 64S content.

As it was previously shown (Fig. 8), the negative zeta potential at pH 9 for the slips with the same solid loading decreased with increasing the 64S content from

0 to 19.9 vol%. The high negative zeta potential of the NH_4PA-adsorbed Y-TZP powder at pH 9 resulted in well dispersed slips with low viscosity and τ_0 values (Figs. 8 and 10). In addition to the electrostatic interaction, the steric interaction of the adsorbed polyelectrolyte contributes to the slip dispersion [14]. The lower negative zeta potential of Y-TZP-64S slips with NH_4PA at pH 9 reduced the electrostatic repulsion between particles, thereby higher viscosity and τ_0 values with respect to Y-TZP slips were found (Fig. 10).

The increase in the particle size of the mixture with increasing the 64S content from 10.5 to 19.9 vol% reduced the amount of NH_4PA adsorbed and consequently the magnitude of negative zeta potential at pH 9, resulting in higher viscosity and yield stress values.

Characterization of green samples

Figure 11 shows the relative green densities of cast samples prepared from 43 vol% slips as a function of the 64S glass content in the mixtures. Calculations of these relative densities were based on the theoretical value of 6.05 g/cm^3 for Y-TZP and the experimental data of 2.70 g/cm^3 for the 64S glass.

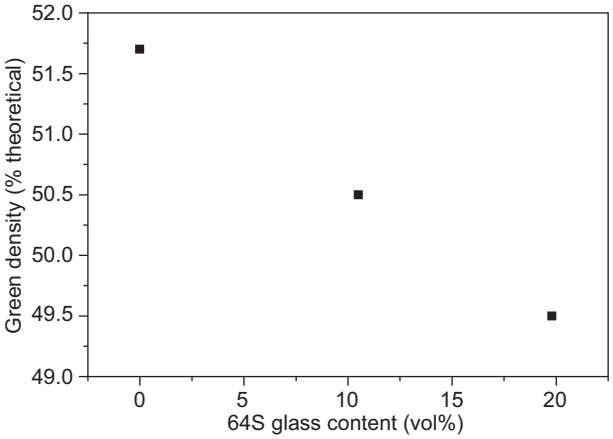

Figure 11. Relative green densities of cast samples prepared from 43 vol% slips as a function of the 64S glass content in the mixtures.

For Y-TZP slips, green density values of about 51.70 % of theoretical density were found; while for 10.5 and 19.9 vol% 64S the green density had values of 50.50 and 49.50 % of theoretical density, respectively. The better slip dispersion of Y-TZP slips resulted in higher green density values, as the 64S content increased the slip viscosity increased and a less dense packing of the samples was achieved (Figs. 10a and 11). The repulsive forces between particles in the stable suspensions and consequently the particles low deposition rate enabled them to pack in an ordered way, obtaining a more dense particle packing. The presence of 64S in the mixtures increased the slip viscosity with NH_4PA resulting in a less dense packing of cast samples.

CONCLUSIONS

The rheological properties of Y-TZP-64S suspensions prepared with two different glass contents (10.5 and 19.9 vol%) with NH_4PA as dispersant, and the particle packing behaviour during slip casting were compared to those of Y-TZP. The substitution of Y-TZP by 64S glass in the mixtures resulted in greater adsorption of NH_4PA; however, the viscosity and yield stress values of Y-TZP-64S slips were higher than those of Y-TZP ones for the solid loadings studied. This behaviour could be explained by the presence of Ca^{2+} ions (high ionic strength) during the aqueous colloidal processing of the mixtures, which reduced the electrostatic repulsion between particles. The increase in the particle size of the mixture with increasing the 64S content from 10.5 to 19.9 vol% reduced the amount of NH_4PA adsorbed, thereby higher viscosity and yield stress values were obtained. The presence of 64S glass in the mixtures resulted in a less dense packing of cast samples.

Acknowledgement

This work was financially supported by CONICET (PIP 0454).

REFERENCES

1. Piconi C., Maccauro G. (1999): Zirconia as a biomaterial. *Biomaterials*, *20*(1), 1-25. doi: 10.1016/S0142-9612(98) 00010-6
2. Hench L. L., Polak J. M. (2002): Third-generation biomedical materials. *Science*, *295*(5557), 1014-1017. doi: 10.1126/science.1067404
3. Ardlin B. J. (2002): Transformation-toughned zirconia for dental inlays, crowns and bridges: chemical stability and effect of low-temperature aging on flexural strength and surface structure. *Dental Materials*, *18*(8), 590-595. doi: 10.1016/S0109-5641(01)00095-1
4. Miyazaki T., Hotta Y., Kunii J., Kuriyama S., Tamaki Y. (2009): A review of dental CAD/CAM: current status and future perspectives from 20 years of experience. *Dental materials journal*, *28*(1), 44-56. doi: 10.4012/dmj.28.44
5. Guazzato M., Albakry M., Ringer S. P., Swain M. V. (2004): Strength, fracture toughness and microstructure of a selection of all-ceramic materials. Part II. Zirconia-based dental ceramics. *Dental materials*, *20*(5), 449-456. doi: 10.1016/j.dental.2003.05.002
6. Sheng X. J., Xu H., Jin Z. H., Wang, Y. L. (2004): Preparation of glass-infiltrated 3Y-TZP/Al_2O_3/glass composites. *Materials Letters*, *58*(11), 1750-1753. doi: 10.1016/j.matlet.2003.10.062
7. Calambás H. L., Albano M. P. (2015): Three different alumina-zirconia composites: sintering, microstructure and mechanical properties. *Materials Science and Engineering: A*, *639*, 136-144. doi: 10.1016/j.msea.2015.05.010
8. Sun Y. H., Zhang Y. F., Guo J. K. (2003): Microstructure and bending strength of 3Y-TZP ceramic by liquid-phase sintering with CAS addition. *Ceramics international*, *29*(2), 229-232. doi: 10.1016/S0272-8842(02)00097-4

9. Santos C., Souza R. C., Habibe A. F., Maeda L. D., Barboza M. J. R., Elias C. N. (2008): Mechanical properties of Y-TZP ceramics obtained by liquid phase sintering using bioglass as additive. *Materials Science and Engineering: A*, *478*(1), 257-263. doi: 10.1016/j.msea.2007.06.009
10. Habibe A. F., Maeda L. D., Souza R. C., Barboza M. J. R., Daguano J. K. M. F., Rogero S. O., Santos C. (2009): Effect of bioglass additions on the sintering of Y-TZP bioceramics. *Materials Science and Engineering: C*, *29*(6), 1959-1964. doi: 10.1016/j.msec.2009.03.006
11. Olhero S., Ganesh I., Torres P., Alves F. J., Ferreira J. M. (2009): Aqueous colloidal processing of ZTA composites. *Journal of the American Ceramic Society*, *92*(1), 9-16. doi: 10.1111/j.1551-2916.2008.02823.x
12. Ganesh I., Sundararajan G., Ferreira J. M. F. (2011): Aqueous slip casting and hydrolysis assisted solidification of $MgAl_2O_4$ spinel ceramics. *Advances in Applied Ceramics*, *110*(2), 63-69. doi: 10.1179/174367610X12804792635260
13. Cesarano III J., Aksay I. A., Bleier A. (1988): Stability of aqueous α-alumina suspensions with poly(methacrylic acid) polyelectrolyte. *Journal of the American Ceramic Society*, *71*(4), 250-255. doi: 10.1111/j.1151-2916.1988.tb05855.x
14. Guldberg-Pedersen H., Bergstrom L. (1988), Stabilizing ceramic suspensions using anionic polyelectrolytes: adsorption kinetics and interparticle forces. *Acta materialia*, *48*(18), 4563-4570. doi: 10.1016/S1359-6454(00)00242-1
15. Hench L.L. (2006): The story of Bioglass. *Journal of Materials Science: Materials in Medicine*, *17*(11), 967-978. doi: 10.1007/s10856-006-0432-z
16. Sepulveda P., Jones J. R., Hench L. L. (2002): In vitro dissolution of melt-derived 45S5 and and sol-gel derived 58S bioactive glasses. *Journal of Biomedical Materials Research Part A*, *61*(2), 301-311. doi: 10.1002/jbm.10207
17. Goh Y. F., Alshemary A. Z., Akram M., Kadir M. R. A., Hussain R. (2013): In vitro study of nano-sized zinc doped bioactive glass. *Materials Chemistry and Physics*, *137*(3), 1031-1038. doi: 10.1016/j.matchemphys.2012.11.022
18. Stábile F. M., Albano M. P., Garrido L. B., Volzone C., De Oliveira P. T., Rosa A. L. (2016): Processing of ZrO_2 scaffolds coated by glass-ceramic derived from 45S5 bioglass. *Ceramics International*, *42*(3), 4507-4516. doi: 10.1016/j.ceramint.2015.11.140
19. Jones J.R. (2013): Review of bioactive glass: From Hench to hybrids. *Acta biomaterialia*,, 9, 4457- 4486. doi: 10.1016/ j.actbio.2012.08.023
20. Elgayar I., Aliev A. E., Boccaccini A. R., Hill, R. G. (2005): Structural analysis of bioactive glasses. *Journal of Non-Crystalline Solids*, *351*(2), 173-183. doi: 10.1016/j.jnoncrysol.2004.07.067
21. Pedone A., Charpentier T., Malavasi G., Menziani, M. C. (2010): New insights into the atomic structure of 45S5 bioglass by means of solid-state NMR spectroscopy and accurate first principles simulations. *Chemistry of Materials*, *22*(19), 5644-5652. doi: 10.1021/cm102089c
22. Hench L. L., Ckark D. E. (1978): Physical chemistry of glass surfaces. *Journal of Non-Crystalline Solids*, *28*(1), 83-105. doi: 10.1016/0022-3093(78)90077-7
23. Goel A., Kapoor S., Rajagopal. R. R., Pascual M. J., Kim H. W., Ferreira J. M. (2012): Alkali-free bioactive glasses for bone tissue engineering: A preliminary investigation. *Acta biomaterialia*, *8*(1), 361-372. doi: 10.1016/j.actbio.2011. 08.026
24. Liu D., Malgham S. G. (1996): Role of polyacrylate in modifying interfacial properties and stability of silicon nitride particles in aqueous suspensions. *Colloids and Surfaces A: Physicochemical and Engineering Aspects*, *110*(1), 37-45. doi: 10.1016/0927-7757(95)03441-2
25. Tari G., Ferreira M. F., Lyckfeldt O. (1998): Influence of the stabilising mechanism and solid loading on slip casting of alumina. *Journal of the European Ceramic Society, 18*(5), 479-486. doi:10.1016/S0955-2219(97)00159-3